COMPENSATOR DESIGN FOR TWIN ROTOR SYSTEMS

A Thesis Submitted to
the Graduate School of Engineering and Sciences of
İzmir Institute of Technology
in Partial Fulfillment of the Requirements for the Degree of

MASTER OF SCIENCE

in Electronics and Communication Engineering

by
Meryem DENİZ

July 2015
İZMİR

We approve the thesis of **Meryem DENİZ**

Examining Committee Members:

Prof. Dr. AYDOĞAN SAVRAN
Department of Electrical and Electronics Engineering
Ege University

Assoc. Prof. Dr. ENVER TATLICIOĞLU
Department of Electrical and Electronics Engineering
İzmir Institute of Technology

Assist. Prof. Dr. BARBAROS ÖZDEMİREL
Department of Electrical and Electronics Engineering
İzmir Institute of Technology

24 July 2015

Assoc. Prof. Dr. Enver TATLICIOĞLU
Supervisor, Department of Electrical and Electronics Engineering
İzmir Institute of Technology

Prof. Dr. M. Salih DİNLEYİCİ
Head of the Department of
Electrical and Electronics Engineering

Prof. Dr. Bilge KARAÇALI
Dean of the Graduate School of
Engineering and Sciences

ACKNOWLEDGMENTS

First of all, I would like to express my deep gratitude to my advisor Assoc. Prof. Dr. Enver Tatlıcıoğlu for his understanding, guidance, encouragement and incredible support in every stage of my thesis study.

I would like to thank committee members for giving me contribution which helped me a lot in revising the thesis.

I would like to express my sincere thanks to Assist. Prof. Dr. Alper Bayrak for his supports, helps and favours.

I would like to thank Assist. Prof. Dr. M. I. Can Dede for his helps and support.

I would like to thank Barış Bıdıklı, Emre Uzunoğlu, Merve Doğan and Ümmügülsüm Seziş for their support.

Also I would like to thank Iztech Robotics laboratory members for their help and favour.

I would like to thank The Scientific and Technological Research Council of Turkey for providing me financial support under grant number $113E147$.

The research leading to this thesis has received funding from IYTE University Research Grant Commission under grant number 2010-IYTE-15.

Finally I would like to thank my parents, Hulusi and Hanife Deniz for their support, prayers and encouragement. Additionally, I would like to thank my brother and my sister, Akan and Hazal Deniz for their good wishes.

ABSTRACT

COMPENSATOR DESIGN FOR TWIN ROTOR SYSTEMS

In this thesis study, modeling and control of the in-house developed twin rotor systems are aimed. Firstly, two input-output models are obtained by using experimentally collected data. One model is obtained as transfer functions in the Laplace domain while the other is a neural network based model. Nextly, lag and lead type compensators are designed and then experimentally verified on the twin rotor system. Specifically, first, lag and lag-lag compensators are designed to obtain a reduced steady state error when compared with proportional controllers. Secondly, lead compensation is discussed to obtain a reduced overshoot. Finally, to make use of their favorable properties at the same time, lag-lead compensators are designed. All the compensators are applied to the twin rotor system in our laboratory.

ÖZET

ÇİFT ROTORLU SİSTEMLER İÇİN DÜZENLEYİCİ TASARIMI

Bu tezde laboratuvarımızda geliştirilmiş olan çift rotorlu sistemin modellenmesi ve denetimi amaçlanmıştır. Deney düzeneğinden toplanan veriler kullanılarak sistemin dikey ve yatay eksende modellenmesi yapay sinir ağı tabanlı modelleme ve transfer fonksiyonu şeklinde ifade edilmektedir. Daha sonra lag ve lead düzenleyiciler tasarlanıp laboratuvarımızda bulunan çift rotorlu sistem üzerine bu düzenleyiciler uygulanmaktadır. Öncelikle lag düzenleyici tasarlayıp sisteme uyguladıktan sonra sistemin kalıcı durum hatasının oransal denetleyiciye göre azaldığı gözlemlenmektedir. Bu ölçüde lag-lag düzenleyici tasarlayıp sistemin kalıcı durum hatasının daha küçük değerlere ulaştığı görülmektedir. Daha sonra lead düzenleyici tasarlayarak sistemin aşma değerinin düşürülmesi amaçlanmaktadır. Hem lag hem de lead düzenleyicinin özelliklerinden faydalanmak için lag-lead düzenleyici tasarlayarak sistemin hem kalıcı durum hatasını azaltmak hem de aşma değerini düşürmek hedeflenmiştir. Tasarlanan tüm düzenleyiciler laboratuvarımızda bulunan çift rotorlu sisteme uygulanarak deneysel gerçeklenme sağlanmaktadır.

TABLE OF CONTENTS

LIST OF FIGURES

Figure **Page**

LIST OF TABLES

Table **Page**

LIST OF SYMBOLS

Y_{mn} ..... Nonlinear system dynamics of MIMO system with ANNs
u_{rn} ..... n^{th} value of r^{th} input of system
y_{mn} ..... n^{th} value of m^{th} output of system
n_u ..... Number of former input signal
n_y ..... Number of former output signal
f ..... Unknown function
T ..... Learning data set
x_k ..... k^{th} input data point at input space
y_k ..... k^{th} output value
$w^1_{j,i}$ ..... Weight from i^{th} input to j^{th} neurons
b^1_j ..... Bias of j^{th} neurons to hidden layer
$w^2_{j,k}$ ..... Weight from j^{th} neurons to k^{th} output
b^2_k ..... Bias from output layer to k^{th} output
$\hat{y}_{kn}$ ..... ANN model of the input-output relation
$h(x)$ ..... Sigmoidal activation function
$d_{j,n}$ ..... Euclidean distance
F ..... Learning error
$Theta$ ..... Vector that contains weights and biases
J_{ANN} ..... Jacobian matrix
e ..... Learning errors vector
$Y_p(s)$ ..... Angular position of pitch axis
$Y_y(s)$ ..... Angular position of yaw axis
$U_p(s)$ ..... Voltages of main motor
$U_y(s)$ ..... Voltages of tail motor
$B_p(s)$ ..... Numerator of polynomial in laplace domain of pitch axis
$F_p(s)$ ..... Denominator of polynomial in laplace domain of pitch axis
$B_y(s)$ ..... numerator of polynomial in laplace domain of yaw axis
$F_y(s)$ ..... Denominator of polynomial in laplace domain of yaw axis
$G_p(s)$ ..... Transfer function of pitch motion
$G_y(s)$ ..... Transfer function of yaw motion
$B_{ps}(s)$ .... Numerator of polynomial in laplace domain of pitch axis of simplified model
$F_{ps}(s)$ .. Denominator of polynomial in laplace domain of pitch axis of simplified model
$G_{ps}(s)$ ..... Transfer function for pitch axis of simplified model

$B_{ys}(s)$ . . . . . Numerator of polynomial in laplace domain of yaw axis of simplified model

$F_{ys}(s)$ . . . Denominator of polynomial in laplace domain of yaw axis of simplified model

$G_{ys}(s)$ . . . . . Transfer function for yaw axis of simplified model

K . . . . . Constant diagonal gain matrix

z_0 . . . . . Zero of system

p_0 . . . . . Pole of system

$e_{p,ss}$ . . . . . Steady state error of pitch axis

$e_{y,ss}$ . . . . . Steady state error of yaw axis

z_1 . . . . . Zero of system

p_1 . . . . . Pole of system

LIST OF ABBREVIATIONS

SISO . . . . . Single Input Single Output
MIMO . . . . . Multi Input Multi Output
CAD . . . . . Computer Aided Design
dof . . . . . Degree of Freedom
RBF . . . . . Radial Basis Function
MPC . . . . . Model Predictive Control
ANNs . . . . . Artificial neural networks
GA . . . . . Genetic Algorithm
DC . . . . . Direct Current
P . . . . . Proportional
I . . . . . Integral
D . . . . . Derivative
PWM . . . . . Pulse Width Modulation
VI . . . . . Virtual Instrument
SSE . . . . . Steady-State Error

CHAPTER 1

INTRODUCTION

In this chapter, firstly the twin rotor system in our laboratory is briefly described. Next, review of the relevant literature on modeling and control of twin rotor systems is presented. Afterwords, motivations behind the thesis study are discussed.

1.1. Twin Rotor System

Twin rotor system is a laboratory setup resembling a simplified helicopter model that moves on both horizontal and vertical axes Dogan (2014), Bayrak et al. (2015). In Figure 1.1, the twin rotor system in our control laboratory which was developed by the funding provided from IYTE University research grant with grant number 2010-IYTE-15 is presented. In Figure 1.1, the two motions of twin rotor system, namely pitch and yaw motions are also shown. In a twin rotor system, two rotors, namely the main rotor and the tail rotor, adjust the angular positions on pitch and yaw axes. The main rotor directly adjusts the movement of the nose of twin rotor system up or down, while the tail rotor causes side to side movement of the nose of the twin rotor system.

Now, subsystems of the twin rotor system are briefly described. The electronic subsystem of the twin rotor system include the main circuit that is constructed by using two encoder readers and two motor driver circuits. Motor driver circuits run the motors in accordance with the controller data received from the computer. Encoder readers obtain position data from the optical encoders as a square wave and calculate quantized angular position. Main circuit receives position and velocity of the twin rotor system and sends these data to the computer while receiving control inputs which are the voltages of two motors from the computer. The electronic components of the system communicate via RS232 serial port. The block diagram of the mentioned process can be seen in Figure 1.2.

LABoratory Virtual Instrument Engineering Workbench (LABVIEW) is used as the software to monitor the twin rotor system and to provide online communication with it. LABVIEW has two sub-interfaces, namely, front panel and block diagram. Front panel is the interactive user interface of LABVIEW which contains push buttons, graphics, many other controls (user inputs) and indicators (program outputs). A screen capture of front

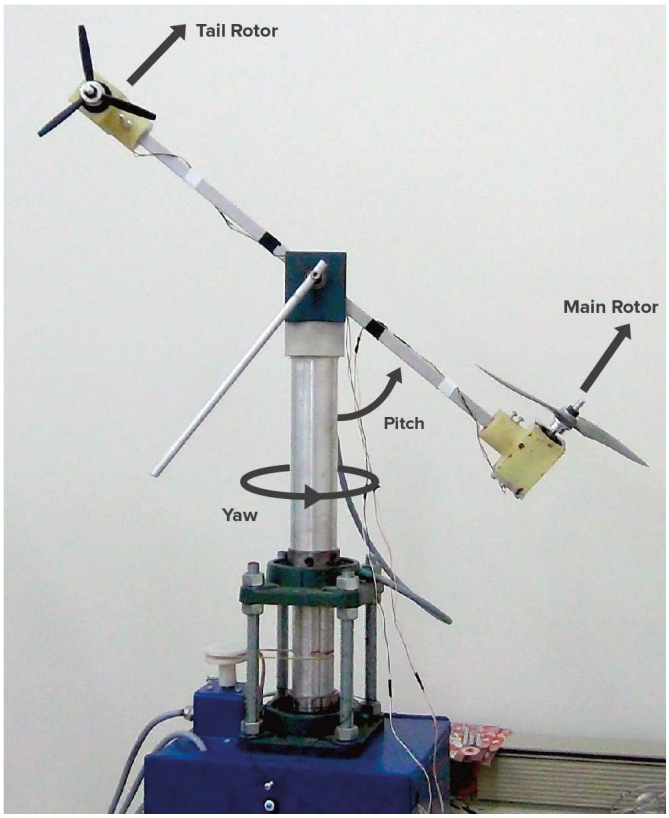

Figure 1.1. The twin rotor system in our laboratory (courtesy of Ilker Tanyer).

panel is shown in Figure 1.3. Block diagram is a code generated with the graphical programming language in LABVIEW. Block diagram consists of sub-programs, functions, constants and loops. A screen capture of the block diagram is given in Figure 1.4.

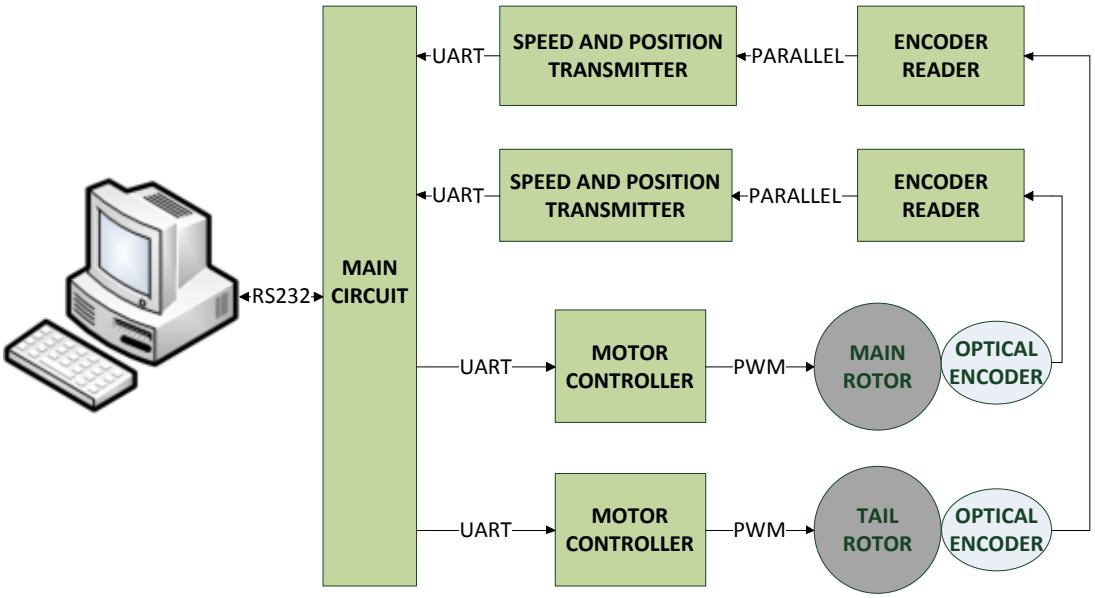

Figure 1.2. The block diagram of the twin rotor system Bayrak et al. (2015) (courtesy of Dr. Enver Tatlicioglu).

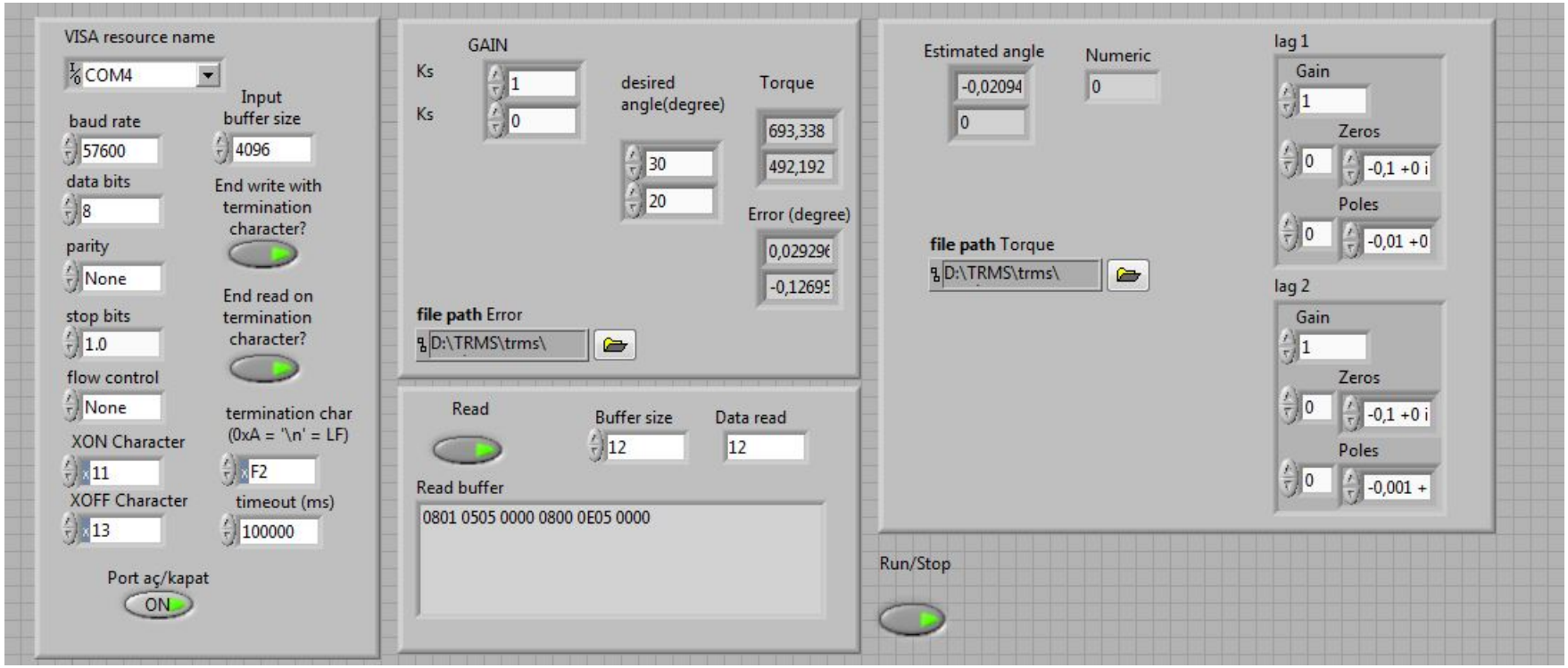

Figure 1.3. Front panel in LABVIEW.

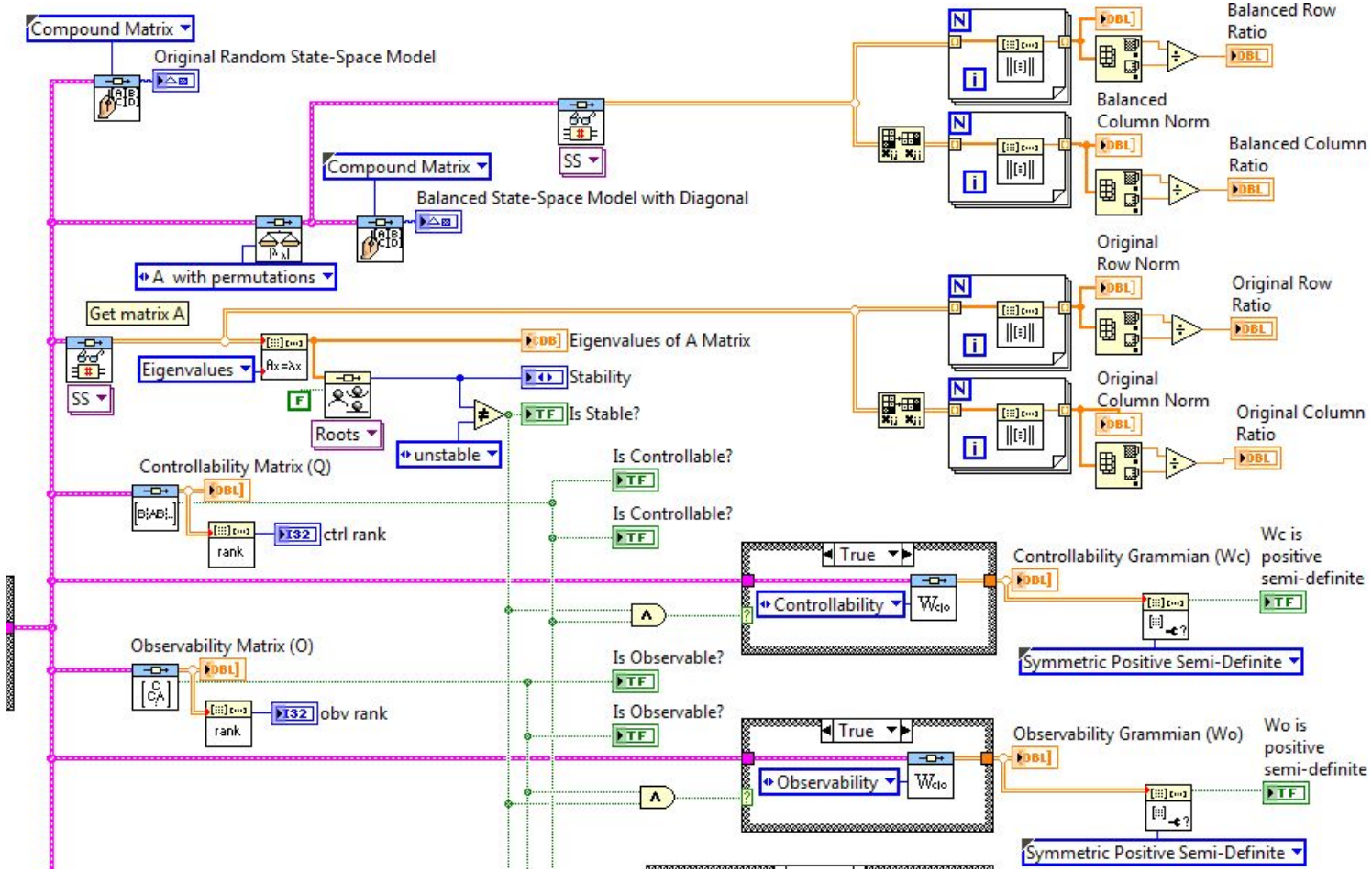

Figure 1.4. Block diagram in LABVIEW.

1.2. Literature Review on Modeling of Twin Rotor Systems

Review of the literature highlights the fact that, a good amount of research was devoted to twin rotor systems. While the name twin rotor system is commonly utilized to describe a 2 degree of freedom (dof) multi input multi output (MIMO) system, some part of past research focused on modeling or control of only one motion of the system. To distinguish these past works, the number of dof is mentioned when required. When not mentioned, a two dof twin rotor system is to be understood.

Some part of this past research focused on modeling of twin rotor systems. These works can roughly be categorized as i) physics-based modeling approaches including energy-based methods such as Newtonian, Euler-Lagrange etc. (*i.e.*, white box system identification), ii) modeling methods utilizing artificial intelligence-like approaches such as neural networks, genetic algorithms, etc (*i.e.*, black box system identification), and iii) some hybrid methods that make use of both of the above methods etc. (*i.e.*, grey box modeling approaches). In Ahmad et al. (2003), modeling of a 1 dof motion of a twin rotor system by using black box system identification technique was presented. In Ahmad et al. (2004), black box system identification was used for modeling a two dof twin rotor system. Rahideh and Shaheed (2008) utilized grey box modeling approach by fusing Newtonian method with genetic algorithms to model a 2 dof twin rotor system. In Toha and Tokhi (2008), artificial neural network based modeling was used to characterize the dynamic behavior of 1 dof motion of a twin rotor system about the vertical plane. They utilized multi-layered perceptron neural networks by using Levenberg-Morquardt based training algorithm and Elman Recurrent neural networks to identify the dynamics of the system. In Shaheed (2005), nonlinear dynamic model of a twin rotor system was developed based on feedforward neural networks by using resilient propagation algorithm to obtain a model via using optimum number of neurons. In Ahmad et al. (2001), a discrete time linear model for a 2 dof twin rotor system was obtained by using parametric modeling and dynamic characterization. In Ahmad et al. (2000), another discrete time linear model was obtained by using black box system identification techniques. Shih et al. (2008) derived an energy-based dynamic model via evaluating the Lagrangian of a twin rotor system. In Ocal and Bingul (2013a), dynamic equations of a 2 dof twin rotor system were obtained with Newtonian methods while unmodeled parameters were obtained by using genetic algorithms. In Rahideh et al. (2008), 1 dof motion of the twin rotor system was modeled via Newtonian and Lagrangian methods and neural networks, and comparative results of these modeling techniques were examined. As a result of

these comparisons, it was observed that neural network based modeling was better in modeling accuracy, while Lagrangian based model had better performance in representing the system dynamics. Reviewing of the relevant literature on modeling twin rotor systems yielded that there is no common agreement on dynamic model for these systems.

1.3. Literature Review on Control of Twin Rotor Systems

Some other past research was devoted to designing controllers for twin rotor systems. These past works can broadly be classified as linear and nonlinear controllers.

1.3.1. Past Works on Linear Controllers and Their Modifications

The linear controllers are based on standard proportional (P), derivative (D), integral (I) feedback controllers. In Shih et al. (2008), a PD controller with gravity compensation and a fuzzy PID controller were designed for set point of control of twin rotor systems. As a result of the comparison of these controllers, it was observed that fuzzy PID controller performed better than the gravity compensated PD controller by decreasing overshoot and steady state error. In Juang et al. (2008), the performance of a PID controller was demonstrated via numerical simulations where the control gains were adjusted by using real value type genetic algorithms. In Juang et al. (2005), a hybrid PID controller was designed for twin rotor systems by combining PID controller with a fuzzy compensator. In the mentioned study, real value type genetic algorithms were utilized to optimize the control gains of the proposed controller. In Juang et al. (2006), a single variable second order grey model was used in design of a switching grey prediction based PID controller where the gains were adjusted by real value genetic algorithms in numerical simulations. Liu et al. (2006) studied to obtain the optimal gains of PID controllers by using model reduced and optimal methods to improve tracking performance and transient response. Rahideh and Shaheed (2006) designed a hybrid fuzzy based PID controller. Comparing the hybrid controller with fuzzy controller and PID controller revealed that hybrid controller has better steady state performance. In Ocal and Bingul (2013b), PID control was used in conjuction with a feedforward inverse model control term for controlling the pitch angle, while a standard PID controller was utilized for controlling the yaw angle. Recently, in Dogan (2014), performances of P, PI, PD and PID controllers were evaluated on the twin rotor system in our laboratory.

1.3.2. Past Works on Nonlinear Controllers

Several nonlinear controllers were designed for twin rotor systems. A nonlinear H_∞ controller was designed by López-Martinez et al. (2005) for twin rotor systems where partial differential equation method was utilized for tuning control gains. Mustafa and Iqbal (2004) used feedback linearization technique for designing controllers for twin rotor systems. In the mentioned study, partial feedback linearization was utilized when a more accurate simulation model of the twin rotor system was used, and exact feedback linearization was the choice for a simplified dynamic model. Lu and Wen (2007) designed a time optimal robust controller for twin rotor systems by decoupling the system into two independent single input single output (SISO) systems. Additionally, the proposed time optimal robust controller was compared with a standard PID controller in settling time and overshoot of the two SISO systems. Karimi and Motlagh (2006) designed a Lyapunov based robust feedback linearization controller. Dong et al. (2008) designed a Radial Basis Function (RBF) neural network controller and a Cerebella Model Articulation controller. Performance of these controllers were evaluated via several numerical simulations. Their simulation results showed that RBF NN controller was better in system performance when compared with standard PID or LQR controllers. López-Martinez and Rubio (2003) proposed a feedback linearization controller for elevation subsystem of a twin rotor system which obviously has 1 input and 2 states (*i.e.*, angular position and velocity). In the design, they used exact input state linearization with a switching law. López-Martinez et al. (2007) designed a nonlinear disturbance rejection method for twin rotor systems by focusing on a tuning procedure for each dof. In Corradini et al. (2011), stabilization by using sliding mode control for discrete time linear systems was investigated. In order to reach this purpose, a discrete-time model of a twin rotor system was used. Rahideh et al. (2007) designed an adaptive nonlinear controller by using Artificial neural networks (ANNs) and genetic algorithms for pitch axis control of a twin rotor system. The controller gains were tuned by using genetic algorithms to improve the tracking performance. Su et al. (2002) designed an inverse complementary sliding mode controller and a terminal sliding mode controller. Recently, in Radac et al. (2014), a data-driven model-free controller and a model-free adaptive controller for twin rotor systems were designed. Tahir et al. (2013) compared switched model predictive control (MPC) with centralized MPC where switched MPC has demonstrated better tracking performance. Witczak et al. (2014) designed a robust predictive fault-tolerant control by using Takagi-Sugeno type fuzzy systems for twin rotor systems. Czajkowski (2014)

focused on estimation of disturbances and then cancelling them by using robust control with echo state network model for twin rotor systems. Alagoz et al. (2013) utilized cube of tracking error in the control design to provide a nonlinear error term in the closed-loop system. In the mentioned study, there was no improvement in steady-state error. Bayrak et al. (2010) designed a robust controller by fusing integral of the signum of the tracking error feedback with a neural network feedforward term where the dynamic model of the twin rotor was considered to be uncertain. In numerical simulations, an improved tracking performance was observed for this controller. Dogan et al. (2012) designed a robust controller and performed numerical simulations by comparing with disturbance and disturbance-free models of a twin rotor system. Recently, in Deniz et al. (2014), different type of robust controllers were designed for twin rotor systems where experimental verification on the twin rotor system in our laboratory was also provided.

1.4. Motivation of Current Research on Twin Rotor Systems

Since the literature review of modeling of twin rotor systems revealed that there is no commonly agreed model for these systems, developing a model for the twin rotor system in our laboratory is aimed. Two input output models, first an artificial neural network based model and next, a transfer function based model are utilizing experimentally collected data.

After carefully reviewing the relevant control literature of twin rotor systems, it was observed that a good amount of research were conducted in designing PID controllers and their extensions in several aspects and also nonlinear controllers. However, there is almost no previous work that designed lag-lead type compensators for twin rotor systems.

In this thesis, this open research problem is investigated. Specifically, lag, lag-lag, lead and lag-lead compensators are designed for controlling both pitch and yaw motions of the twin rotor system. Lag compensators without changing the transient characteristics of a system much, have a significant decreasing effect on the steady-state error. Lag lag compensators reduced the steady state error even further are more successful in reducing steady state error than lag compensator. Where lag-lag compensators have a stronger similar effect as well. Lead compensators are usually preferred to change the transient behavior of systems. Lag and lead type compensators are designed and then experimentally tested on the twin rotor system in our laboratory.

1.5. Organization of This Thesis

The rest of this thesis is organized as follows. In Chapter 2, two modeling approaches are given. Firstly, obtained from experimentally collected data, an input output model is presented by using artificial neural networks. Secondly, also obtained from experimentally collected data, transfer functions of both pitch and yaw motions are given. In Chapter 3, properties of lag compensator is given along with simulation results on the transfer function model of a twin rotor system and experimental results on the twin rotor system in our laboratory. In Chapter 4, design and verification of lead compensators are presented. In Chapter 5, lag-lead compensators are designed and experimentally verified on the twin rotor system. Finally, in Chapter 6, concluding remarks are given along with possible future works.

CHAPTER 2

MODELING OF TWIN ROTOR SYSTEMS

In this chapter, two approaches for developing input-output models of the twin rotor system in our laboratory are presented. The first approach is based on obtaining the input-output relation by using ANNs. In the second approach, transfer functions of motions on both pitch and yaw axes are obtained. In both modeling approaches, experimentally collected data are utilized.

2.1. Modeling of Twin Rotor System by Using Artificial Neural Networks

ANNs are artificial systems that are modeled by mimicking the working principle of the human brain. These systems consist of pathways between the layers consisting of neurons which allow the data transmission. An ANN model can be developed by using existing information about the system to predict its future behavior with high precision by using the developed model.

In this study, the input output relation of the twin rotor system in our laboratory is obtained by using ANNs. When compared with the existing literature, main advantage of this modeling approach is that multi-input multi-output ANN structure is used. As a result of this approach, the cross coupling effects between the rotors are taken into consideration. Thus, we sincerely believe that the obtained input-output model demonstrates a close behavior to the real system in the region of operation that the data were collected.

2.1.1. Modeling, Prediction, and Jacobian Calculation

Nonlinear behaviour of a MIMO system defined with ANNs is given as follows

$$Y_{mn} = f\left(u_{1n}, \cdots, u_{1(n-n_u)}, \cdots, u_{r(n-n_u)}, y_{1(n-1)}, \cdots, \ y_{1(n-n_y)}, \cdots, y_{m(n-n_y)}\right) \quad (2.1)$$

where $u_{rn} \in \mathbb{R}$ is n^{th} value of r^{th} input of the system, $y_{mn} \in \mathbb{R}$ is n^{th} value of m^{th}

output, the number of former input signals and output signals are n_u and n_y, respectively. In (2.1), the unknown function $f \in \mathbb{R}$ can be obtained by applying the available learning data set to ANN system as

$$\begin{aligned} T &= \{u_{1k}, \cdots, u_{1(k-n_u)}, \cdots, u_{r(k-n_u)}, y_{1(k-1)}, \cdots, \\ &\quad y_{1(k-n_y)}, \cdots, y_{m(k-n_y)}; y_{1k}, \cdots, y_{mk}\}_{k=n}^{k=n+N} \\ &= \{x_k, y_k\}_{k=1}^{k=N} \end{aligned} \tag{2.2}$$

where $x_k \in \mathbb{X} \subseteq \mathbb{R}^{[rn_u+m(n_y+1)]}$ denotes k^{th} input data point at input space, while $y_k \in \mathbb{Y} \subseteq \mathbb{R}^m$ denotes the related output value. A model that represents the approximate input–output relation of the system will be obtained by using the feedforward single layer ANN structure given in Figure 2.1.

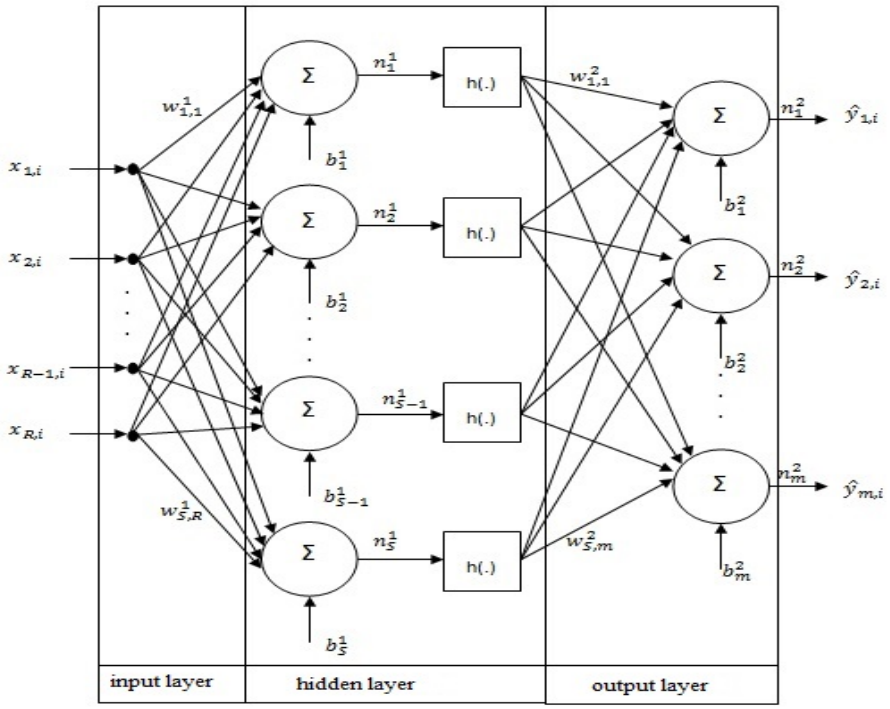

Figure 2.1. ANN structure

.

In this structure, R denotes the number of inputs and it is defined as $R \triangleq rn_u + m(n_y + 1)$, $w^1_{j,i}$ is the weight from i^{th} input to j^{th} neurons, b^1_j denotes the bias of j^{th} neurons to hidden layer, $w^2_{j,k}$ is the weight from j^{th} neurons to k^{th} output and b^2_k is the bias from output layer to k^{th} output. ANN model of the system is obtained by optimizing

these weights and biases at each iteration until the best relation between the inputs and the outputs is provided. After this point, ANN predicts the outputs of the system according to

$$\hat{y}_{kn} = \sum_{k=1}^{m} \left(\sum_{j=1}^{S} w_{k,j}^{2} h\left(d_{j,n}\right) + b_{k}^{2} \right) \tag{2.3}$$

where $h\left(x\right) \in \mathbb{R}$ is the sigmoidal activation function and it is chosen as $\frac{\left(e^{x}-e^{-x}\right)}{\left(e^{x}+e^{-x}\right)}$. Also, S is used to specify the number of neurons at the hidden layer. In (2.3), $d_{j,n} \in \mathbb{R}$ can be obtained as

$$d_{j,n} = \sum_{k=1}^{R} \left(\sum_{i=0}^{nu} w_{j,i}^{1} u_{k(n-i)} \right) + \sum_{l=1}^{m} \left(\sum_{i=1}^{ny} w_{j,n_u+i+1}^{1} y_{l(n-i)} \right) + b_{j}^{1}. \tag{2.4}$$

Minimizing the following error equation is the main principle of ANN modeling

$$F = \sum_{l=1}^{m} \sum_{k=1}^{N} \left(y_{lk} - \hat{y}_{lk}\right)^{2}. \tag{2.5}$$

In order to minimize the error function in (2.5), adjustable parameters are optimized via the Levenberg-Marquardt optimization rule as

$$\Theta^{new} = \Theta^{old} - \left(J_{ANN}^{T} J_{ANN} + \mu I_{R}\right)^{-1} J_{ANN}^{T} e \tag{2.6}$$

where $e \in \mathbb{R}^{(M\times N)\times 1}$ is the vector that contains learning error and is defined as

$$\begin{aligned} e &= \begin{bmatrix} e_{11} & \cdots & e_{1N} & \cdots e_{M1} & \cdots & e_{MN} \end{bmatrix}^{T} \\ &= \begin{bmatrix} y_{11}-\hat{y}_{11} & \cdots & y_{N1}-\hat{y}_{N1} & \cdots & y_{M1}-\hat{y}_{M1} & \cdots & y_{MN}-\hat{y}_{MN} \end{bmatrix}^{T}. \end{aligned} \tag{2.7}$$

In (2.6), $\Theta \in \mathbb{R}^{R\times 1}$ is the vector that contains weights and biases and is defined as follows

$$\begin{aligned} \Theta &= \begin{bmatrix} w_{1,1}^{1} & \cdots & w_{s,n_u+N_y+1}^{1} & b_{1}^{1} & \cdots & b_{s}^{1} & w_{1,1}^{2} & \cdots & w_{1,s}^{2} & \cdots & w_{m,s}^{2} & b_{1}^{2} & \cdots & b_{m}^{2} \end{bmatrix}^{T} \\ &= \begin{bmatrix} \theta_{1} & \cdots & \theta_{R} \end{bmatrix}^{T} \end{aligned} \tag{2.8}$$

and $J_{ANN} \in \mathbb{R}^{(M\times N)\times R}$ is a Jacobian matrix which has the following structure

$$J_{ANN} = \begin{bmatrix} \frac{\partial e_{11}}{\partial \theta_{1}} & \cdots & \frac{\partial e_{11}}{\partial \theta_{R}} \\ \vdots & \ddots & \vdots \\ \frac{\partial e_{MN}}{\partial \theta_{1}} & \cdots & \frac{\partial e_{MN}}{\partial \theta_{R}} \end{bmatrix}. \tag{2.9}$$

ANN model of the system can be completed by reducing the value of the error function given in (2.5) to a desired level. After obtaining a proper model for the system, the future behavior can be estimated via (2.3) and (2.4).

2.1.2. ANN Model of Twin Rotor System

In this study, input-output relation of the twin rotor system is modeled by using ANNs. Necessary input-output data for this modeling approach are provided from the experimental setup in our laboratory. The voltage values of motor are used as the inputs while the angular positions of pitch and yaw axes are used as the outputs. It is clear that better model accuracy is obtained by using more and diverse data from different points of input and output spaces. After selecting appropriate amount of input and output data, the best representation of the real system can be obtained successfully. As a result of necessary selection process, 3000 data points obtained from experiments are considered sufficient for the ANN based modeling. The best decomposition ratios were obtained via trial and error method and found as $\%70$ and $\%30$ for learning and validation processes, respectively. As a result, 2100 data points were used for the learning process while remaining 900 data points were used for the validation process. It is highlighted that above mentioned data were used in a random manner for avoiding memorizing. The number of former inputs and outputs of the system are found as $n_u = 5$ and $n_y = 5$ again by using trial and error.

Another important part of ANN based modeling is obtaining the optimal number of neurons. Too much neurons mean relatively large weights and biases which usually results in slowing down modeling and prediction processes. To obtain the best value for number of neurons, the algorithm was run 1000 times from 1 neuron to 330 neurons. For every number of neurons in the mentioned interval, learning and validation error is shown in Figures 2.3 and 2.4, respectively, from which, it is clear that there are no big changes in error values after 14 neurons as shown in Figure 2.2. According to these results, 14 neurons gave the satisfactory modeling performance.

The outcome of the ANN based modeling are discussed. In Figure 2.5, corresponding input values to the output values obtained from the model are given. From this figures, it is demonstrated that modeling approach have reached its goal and an ANN based model representing the twin rotor system in our laboratory with high accuracy was obtained.

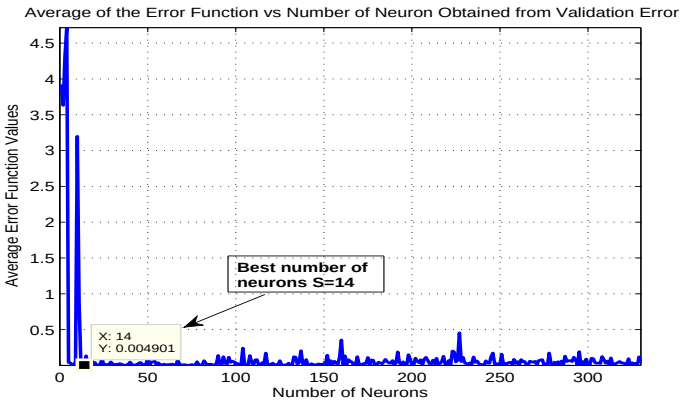

Figure 2.2. Average values of error functions

2.2. Transfer Functions for Pitch and Yaw Motions of Twin Rotor System

In this section, transfer functions of pitch and yaw motions are obtained by using input and output data obtained from the experiments performed on the twin rotor system. The input data consists of the voltages supplied to the motors while the output data includes the angular pitch and yaw positions. Matlab System Identification Toolbox[1] is utilized to obtain the transfer functions.

The transfer function is considered to be of the following form

$$\begin{bmatrix} Y_p(s) \\ Y_y(s) \end{bmatrix} = \begin{bmatrix} \frac{B_p(s)}{F_p(s)} & 0 \\ 0 & \frac{B_y(s)}{F_y(s)} \end{bmatrix} \begin{bmatrix} U_p(s) \\ U_y(s) \end{bmatrix} \tag{2.10}$$

where $Y_p(s)$, $Y_y(s)$ are the angular positions of the pitch and yaw axes, respectively, $U_p(s)$, $U_y(s)$ are the supply voltages of the main motor and the tail motor respectively, and $B_p(s)$, $F_p(s)$, $B_y(s)$, $F_y(s)$ are polynomials in the Laplace domain, and transfer functions of pitch and yaw axes are expressed as $\frac{B_p(s)}{F_p(s)}$ and $\frac{B_y(s)}{F_y(s)}$, respectively. Matlab System Identification Toolbox returned the following for the pitch motion

$$B_p(s) = 25.49s^2 + 559.2s + 0.01386 \tag{2.11}$$

$$F_p(s) = s^3 + 0.9214s^2 + 10.08s + 0.007895 \tag{2.12}$$

[1] http://www.mathworks.com/products/sysid/

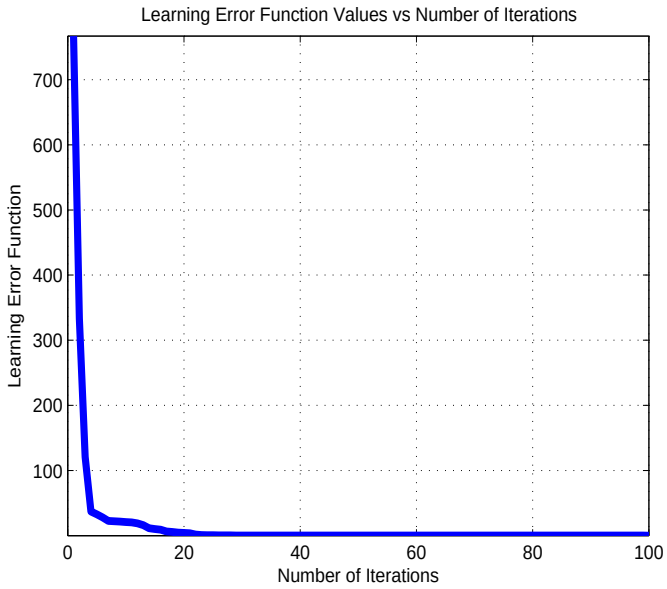

Figure 2.3. Learning error values which are obtained during the modeling

which yield the following transfer function

$$G_p(s) = \frac{25.49s^2 + 559.2s + 0.01386}{s^3 + 0.9214s^2 + 10.08s + 0.007895} \tag{2.13}$$

and the following for the yaw motion

$$B_2(s) = 1.705s^2 + 13.11s + 0.8412 \tag{2.14}$$

$$F_2(s) = s^3 + 3.327s^2 + 12.72s + 0.669 \tag{2.15}$$

which results in the following transfer function

$$G_y(s) = \frac{1.705s^2 + 13.11s + 0.8412}{s^3 + 3.327s^2 + 12.72s + 0.669}. \tag{2.16}$$

For both motions, the order of the numerators are 2 while the order of the denominators are 3. This makes perfect sense in the sense that after considering that the relative degree between the torque provided by the motor and the angular position is 2 and the relative degree between the torque provided by the motor and the supply voltage is 1, and thus a third order polynomial was expected on the denominator of the transfer functions.

Poles and zeros of the transfer function of the pitch motion are found as

$$\begin{aligned} \text{poles} &= \Big\{-0.4603 + 3.1412j, \quad -0.4603 - 3.1412j, \quad -0.0008\Big\} \\ \text{zeros} &= \Big\{-21.9380, \quad -0.000024\Big\} \end{aligned} \tag{2.17}$$

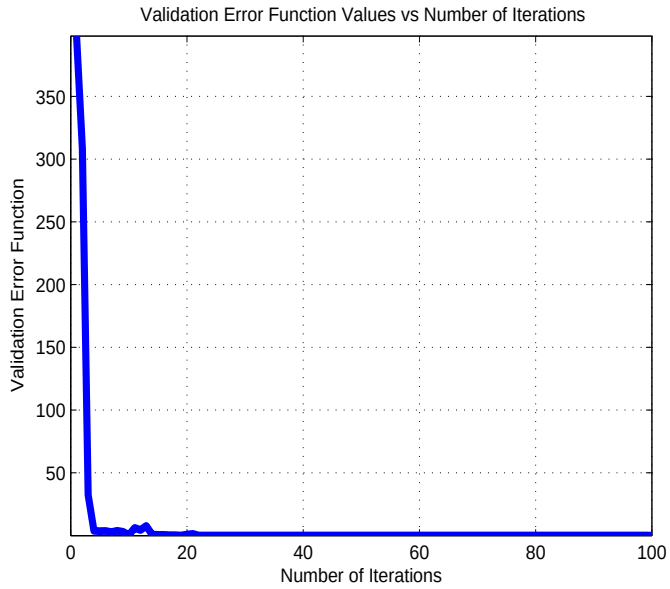

Figure 2.4. Validation error values which are obtained during the modeling

while the ones for the yaw motion are found as

$$\begin{aligned} \text{poles} &= \left\{-1.6368 + 3.1410j, \quad -1.6368 + 3.1410j, \quad -0.0533\right\} \\ \text{zeros} &= \left\{-7.6244, \quad -0.0647\right\}. \end{aligned} \tag{2.18}$$

Since for both motions the constant terms in numerator and denominator are relatively small when compared with the parameters of powers of s, they can be assumed as zero to yield the following for the pitch motion

$$B_{p_s}(s) = 25.49s + 559.2 \tag{2.19}$$

$$F_{p_s}(s) = s^2 + 0.9214s + 10.08 \tag{2.20}$$

where the simplified transfer function for pitch axis now has the form

$$G_{p_s}(s) = \frac{25.49s + 559.2}{s^2 + 0.9214s + 10.08} \tag{2.21}$$

and following for the yaw motion

$$B_{y_s}(s) = 1.705s + 13.11 \tag{2.22}$$

$$F_{y_s}(s) = s^2 + 3.327s + 12.72. \tag{2.23}$$

where the simplified transfer function for yaw axis is given as

$$G_{y_s}(s) = \frac{1.705s + 13.11}{s^2 + 3.327s + 12.72}. \tag{2.24}$$

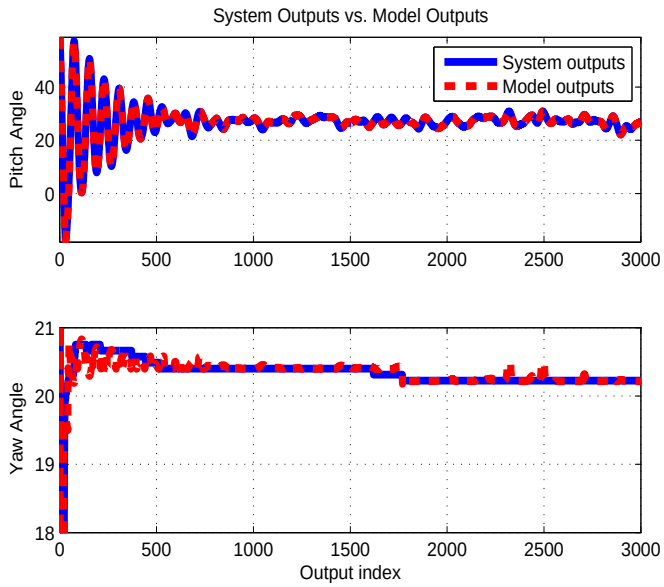

Figure 2.5. ANN output corresponds to the system output

For the simplified case, poles and zero of the transfer function of the pitch motion are found as

$$\begin{aligned} \text{poles} &= \Big\{-0.4607 + 3.1413j, \quad -0.4607 - 3.1413j\Big\} \\ \text{zeros} &= \Big\{-21.9380\Big\} \end{aligned} \tag{2.25}$$

while for the yaw motion poles and zero are found as

$$\begin{aligned} \text{poles} &= \Big\{-1.6635 + 3.1548j, \quad -1.6635 - 3.1548j\Big\} \\ \text{zeros} &= \Big\{-7.6891\Big\}. \end{aligned} \tag{2.26}$$

Comparing (2.17) with (2.25) and (2.18) with (2.26) reveals that the above simplification has a minor affect which can indeed be ignored. This simplification has a physical interpretation as well. The transfer function of a motor relating the supply voltage to the torque produced is sometimes considered as constant. When this is the case a second order transfer function is obtained.

2.3. Conclusions

In this chapter, two input output models were developed for the twin rotor system in our laboratory. The first one was an input-output model which was obtained in the

time domain via ANNs and the second one was a Laplace domain modeling which was obtained by utilizing Matlab System Identification Toolbox. As a result, two different transfer functions were obtained for pitch and yaw motions which will later be utilized in numerical simulations.

CHAPTER 3

LAG COMPENSATION

In this chapter, first, lag type compensation along with its main properties are given. Next, steady state error comparisons are given for lag and lag-lag compensators with a proportional controller. Results of experiments performed on the twin rotor system are presented followed by concluding remarks.

3.1. Definition and Properties of Lag Compensators

The main principle of the lag compensator is based on phase lagging of a sinusoidal input signal Franklin et al. (1998). Necessary phase delays at high frequencies are provided by utilizing this main principle. Lag compensator is a compensator type that is used instead of P or PI controllers. Some disadvantages of the mentioned controllers like integrator windup due to actuator saturation can be eliminated in assistance of a lag compensator. Although, lag compensators have some disadvantages like reduced gain crossover frequency, due to weakening effect, increased rise and settling time that cause worse system stability and transient response, it is considered as one of the most important solutions for improving steady state error. This important property of lag compensators will be utilized throughout this thesis study.

General structure of the transfer function of lag compensator is expressed in two different forms that are given as

$$D(s) = K\frac{s - z_0}{s - p_0} \tag{3.1}$$

$$D(s) = \frac{a_1 s + a_0}{b_1 s + 1} \tag{3.2}$$

where K, z_0, p_0 are gain, zero and pole of the compensator, respectively, and a_0, a_1, b_1 are constants that can be obtained from K, z_0, and p_0, or vice versa. In general, designs are usually based on a transfer function of the form

$$D(s) = K\frac{s + a}{s + b} \tag{3.3}$$

which is very similar to (3.1) with $a = -z_0$ and $b = -p_0$.

In (3.1), pole p_0 must be closer to the origin than the zero z_0 which is the mandatory condition of lag compensator design (*i.e.*, $|p_0| < |z_0|$). Pole-zero location of the lag compensator should be adjusted appropriately to reduce possible negative effects of the lag compensator to the transient response which can be provided by selecting pole and zero locations in a way not to change the root locus much.

3.2. Lag-Lag Compensator

When the performance of a lag compensator is not at the desired level in reducing steady state error an alternative is to utilize a double lag compensator in the sense that

$$D(s) = K\left(\frac{s+a}{s+b}\right)^2 \tag{3.4}$$

which is commonly called as lag-lag compensator.

3.3. Comparison of Proportional Controller with Lag and Lag-Lag Compensators in Steady State Error

To demonstrate the effectiveness of a lag compensator, the steady state error is calculated when a proportional control is applied with a step reference input for only the pitch motion. Specifically, let $D_p(s) = K = 10$ and $R_p(s) = \frac{30}{s}$. The closed-loop transfer function is obtained as

$$\frac{Y_p(s)}{R_p(s)} = \frac{KG_p(s)}{1 + KG_p(s)} \tag{3.5}$$

where $G_p(s)$ in (2.13) is to be utilized. The angular position tracking error in pitch axis is defined as

$$E_p(s) \triangleq R_p(s) - Y_p(s) \tag{3.6}$$

and substituting (3.5) results in

$$E_p(s) = \frac{1}{1 + KG_p(s)} R_p(s). \tag{3.7}$$

By using the Final Value Theorem Dorf and Bishop (1998), the steady state error can be obtained as

$$\begin{aligned} e_{p,ss} &= \lim_{t\to\infty} e_p(t) \\ &= \lim_{s\to 0} sE_p(s) \end{aligned} \tag{3.8}$$

to which substituting (3.7), $K = 10$ and $R_p(s) = \frac{30}{s}$ yields

$$e_{p,ss} = \frac{30}{1 + K\frac{0.01386}{0.007895}} = 1.616 \text{ degrees.}$$

It is further noted that increasing K results in a decreased steady state error.

Similarly, the steady state error analysis of a proportional controller applied to the tail motor for the yaw motion to track a step reference input is discussed. Specifically, let $D_y(s) = K = 3000$ and $R_y(s) = \frac{20}{s}$. Similarly, the closed-loop transfer function for the yaw motion is obtained as

$$\frac{Y_y(s)}{R_y(s)} = \frac{KG_y(s)}{1 + KG_y(s)} \tag{3.9}$$

where $G_y(s)$ in (2.16) is to be utilized. The angular position tracking error in yaw axis is defined as

$$E_y(s) \triangleq R_y(s) - Y_y(s) \tag{3.10}$$

to which substituting (3.10) yields

$$E_y(s) = \frac{1}{1 + KG_y(s)} R_y(s). \tag{3.11}$$

Via utilizing the Final Value Theorem, the steady state error is found as

$$\begin{aligned} e_{y,ss} &= \lim_{t\to\infty} e_y(t) \\ &= \lim_{s\to 0} sE_y(s) \end{aligned} \tag{3.12}$$

Substituting $D_y(s) = K = 3000$ and $R_y(s) = \frac{20}{s}$ yields in

$$e_{y,ss} = \frac{20}{1 + K\frac{0.8412}{0.669}} = 0.0053005 \text{ degrees}$$

From the above structure, it is clear that when K increases steady state error decreases. Applying the same proportional controllers when the simplified transfer functions in (2.21) and (2.24) are utilized while considering the same reference inputs yields

$$e_{p,ss} = 0.0540 \text{ degrees}$$

$$e_{y,ss} = 0.006466 \text{ degrees.}$$

Now, steady state error performances of a lag compensator for the same step reference inputs for pitch and yaw motions are examined. Specifically, for the pitch motion, let $D_p(s) = K\frac{s+a}{s+b}$ with $K = 10$ (*i.e.*, same gain as in the proportional controller) and

$a = 0.1$ and $b = 0.01$ which is a standard lag compensator. The reference input is chosen same as before (*i.e.*, $R_p(s) = \frac{30}{s}$). The transfer function now has the following structure

$$\frac{Y_p(s)}{R_p(s)} = \frac{D_p(s)G_p(s)}{1 + D_p(s)G_p(s)} \tag{3.13}$$

where the angular position tracking error in pitch axis is found as

$$E_p(s) = \frac{1}{1 + K\frac{s+a}{s+b}G_p(s)}R_p(s). \tag{3.14}$$

After following similar steps, the steady state error is obtained as

$$e_{p,ss} = 0.169 \text{ degrees}$$

For the yaw axis, let $D_y(s) = K\frac{s+a}{s+b}$ with $K = 3000$ (*i.e.*, which is same as the gain of the proportional controller) and with $a = 0.1$ and $b = 0.001$. The transfer function is obtained as

$$\frac{Y_y(s)}{R_y(s)} = \frac{D_y(s)G_y(s)}{1 + D_y(s)G_y(s)} \tag{3.15}$$

with the output tracking error is found as

$$E_y(s) = \frac{1}{1 + K\frac{s+a}{s+b}G_y(s)}R_y(s). \tag{3.16}$$

The steady state error is now found as

$$e_{y,ss} = 0.0000530 \text{ degrees.}$$

When the above lag compensators are considered as the control inputs to the simplified transfer functions in (2.21) and (2.24) with the same reference inputs, we obtain

$$e_{p,ss} = 0.005406 \text{ degrees}$$

$$e_{y,ss} = 0.00006468 \text{ degrees.}$$

When lag-lag compensators for pitch and yaw axes of the form $D_p(s) = 10(\frac{s+0.1}{s+0.01})^2$ and $D_y(s) = 3000(\frac{s+0.1}{s+0.001})^2$ are applied to the system with transfer functions in (2.13) and (2.16), steady state errors on pitch and yaw axes are obtained as

$$e_{p,ss} = 0.0170 \text{ degrees}$$

$$e_{y,ss} = 5.30 \times 10^{-7} \text{degrees.}$$

To the simplified model, steady state errors are obtained for both axes which are

$$e_{p,ss} = 0.00054076 \text{ degrees}$$

$$e_{y,ss} = 0.0000006468 \text{ degrees.}$$

As numerically demonstrated in this section (see Table 3.1), lag and lag-lag compensators provide a significant decreasing effect on the steady state error when compared with a proportional controller.

Table 3.1. Comparison of steady state errors for pitch and yaw axes for proportional controller and lag and lag-lag compensator

	Proportional controller		Lag compensator		Lag-lag compensator	
Transfer Function	pitch	yaw	pitch	yaw	pitch	yaw
Third order model	1.616	5.3×10^{-3}	0.1699	5.3×10^{-5}	0.0170	5.3×10^{-7}
Simplified model	0.054	6.4×10^{-3}	5.4×10^{-3}	6.4×10^{-5}	5.4×10^{-4}	6.4×10^{-7}

3.4. Experimental Results

In this section, the experimental results obtained from the twin rotor system are presented. In these experiments, the performances of proportional controller, lag compensator and lag-lag compensator are compared. These controllers are evaluated first for set-point control of the pitch motion and then for set-point control of both pitch and yaw motions. The results of these experiments are presented in a comparative manner by calculating the steady state error while one of these results is presented graphically. Specifically, angular pitch position for proportional controller with gain of 10 for only main motor is given in Figure 3.1. Result derived when lag compensator of form $10\frac{s+0.1}{s+0.01}$ is applied on main motor, is shown in Figure 3.2. $10(\frac{s+0.1}{s+0.01})^2$ form of lag-lag compensator is applied on main motor to obtain result which is shown in Figure 3.3. Secondly, angular pitch and yaw positions for a proportional controller with gains of 10 and 3000 for main and tail motors, respectively, is given in Figure 3.4. Results obtained when lag compensators of the form $10\frac{s+0.1}{s+0.01}$ and $3000\frac{s+0.1}{s+0.001}$ are applied to main and tail motors, respectively, are shown in Figure 3.5. Results from evaluation of lag-lag compensators $10(\frac{s+0.1}{s+0.01})^2$ and $3000(\frac{s+0.1}{s+0.001})^2$are applied on both main and tail motors, respectively, are given in Figure 3.6.

As expected with the steady state error analysis, the lag-lag compensator performed best among the three compensators while proportional controller was the worst

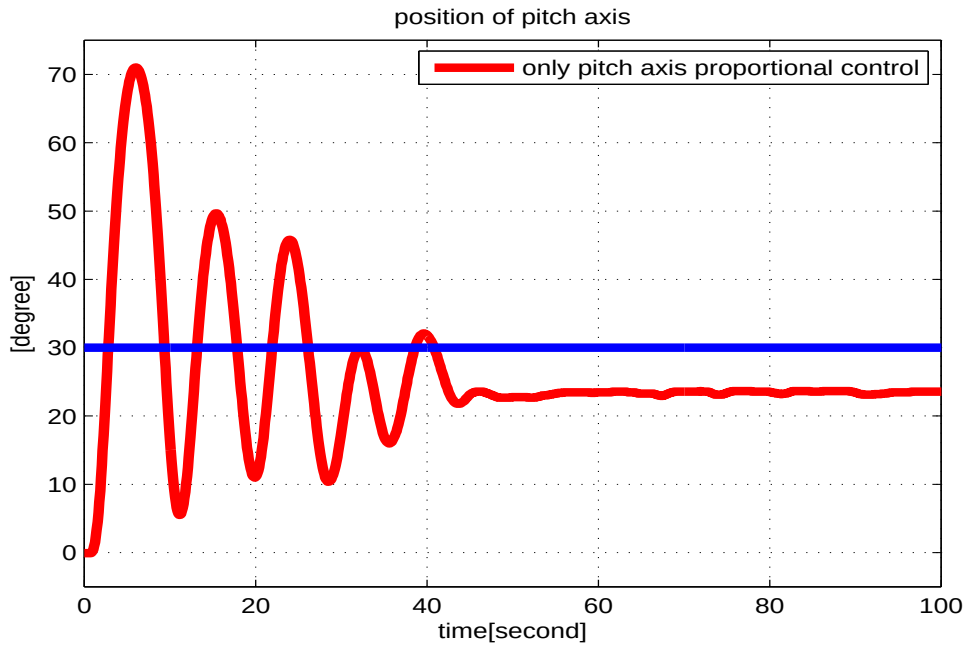

Figure 3.1. Angular pitch (top) position for proportional controller with gain 10 for main motor.

in steady state error. It is clear that from Figures 3.4 and 3.5, the steady state error is improved with the lag compensator when compared with the proportional controller. In Figure 3.6, it is shown that the steady state error improves with lag-lag compensator.

In Table 3.2, steady state errors obtained from several experiments, after applying different lag and lag-lag compensators for set-point control of only pitch angular position, are presented. The zero and the constant gain were same for all the lag compensators and the location of the pole was varied and no control was applied to the tail motor.

As expected, the lowest steady state error was observed when the zero-pole ratio was highest and when the zero-pole ratio was decreased the steady state error increased. All of these steady state errors were less than the steady state errors obtained with proportional control. It can also be observed that the lag-lag compensator as an improved performance compared to the lag compensator in steady state error.

In Table 3.3, steady state errors obtained after applying different lag and lag-lag compensators to both motors of the twin rotor system are given. In these experiments, the compensators applied to the tail rotor were kept the same since satisfactory performance was obtained and thus only the compensators applied to the main rotor were varied.

When the zero-pole ratio of the lag and lag-lag compensators were the highest, lowest steady state error in both axes was observed and as the zero-pole ratio is decreased

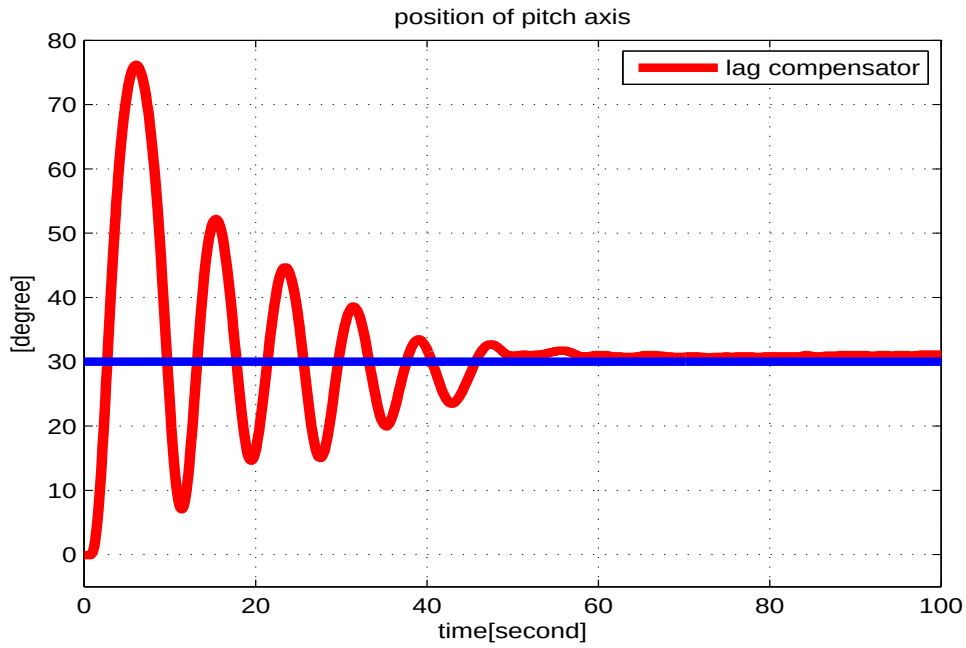

Figure 3.2. Angular pitch (top) position for lag compensator of the form $10\frac{s+0.1}{s+0.01}$ applied to a main motor.

the steady state error increased.

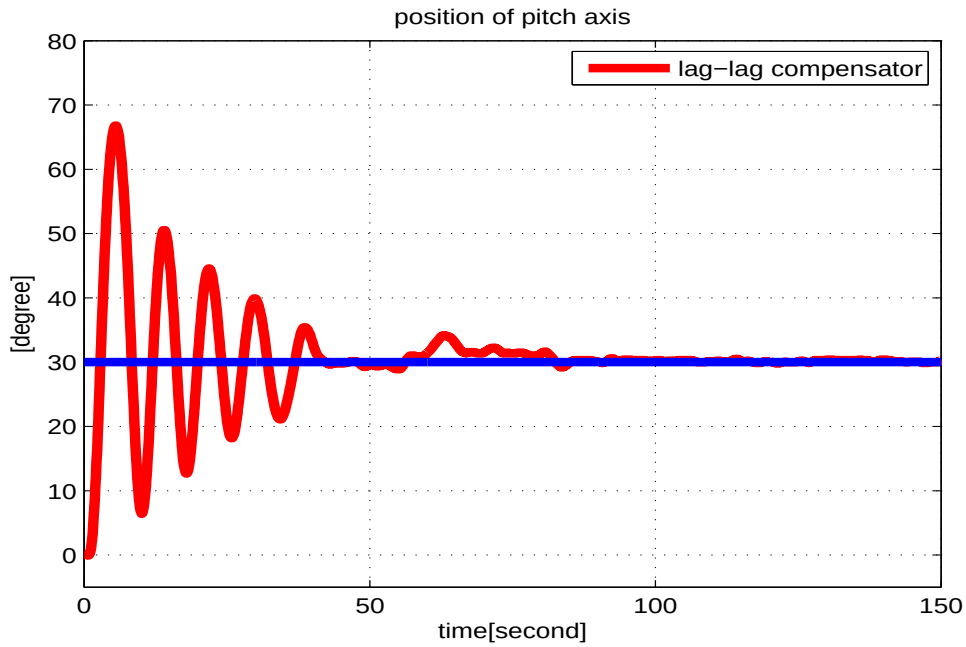

Figure 3.3. Angular pitch (top) position for lag-lag compensators of the form $10(\frac{s+0.1}{s+0.01})^2$ applied to main motor.

Table 3.2. Comparison of steady state errors of angular pitch position when different controllers applied only on the main motor.

Controller			Steady state error		
proportional	lag	lag-lag	proportional	lag	lag-lag
main motor			pitch axis		
10	$10\frac{s+0.1}{s+0.01}$	$10(\frac{s+0.1}{s+0.01})^2$	3.545	1.436	0.117
10	$10\frac{s+0.1}{s+0.02}$	$10(\frac{s+0.1}{s+0.02})^2$	3.545	1.963	0.557
10	$10\frac{s+0.1}{s+0.03}$	$10(\frac{s+0.1}{s+0.03})^2$	3.545	2.49	1.611
10	$10\frac{s+0.1}{s+0.04}$	$10(\frac{s+0.1}{s+0.04})^2$	3.545	2.93	2.139
10	$10\frac{s+0.1}{s+0.05}$	$10(\frac{s+0.1}{s+0.05})^2$	3.545	3.457	2.578

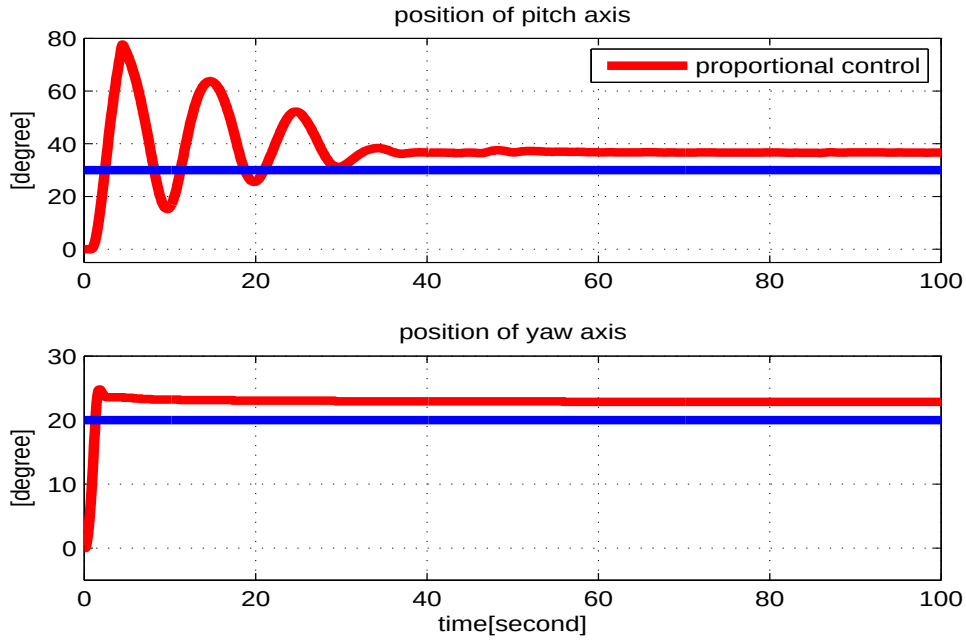

Figure 3.4. Angular pitch (top) and yaw (bottom) positions for proportional controllers with gains 10 and 3000 for main and tail motors, respectively.

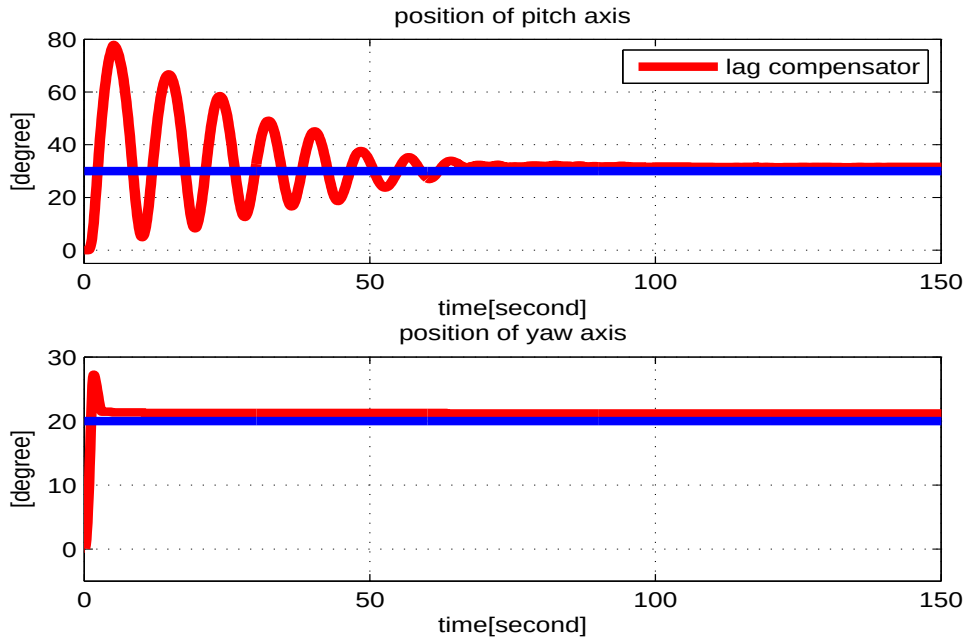

Figure 3.5. Angular pitch (top) and yaw (bottom) positions for lag compensators of the form $10\frac{s+0.1}{s+0.01}$ and $3000\frac{s+0.1}{s+0.001}$ applied to a main and tail motors, respectively.

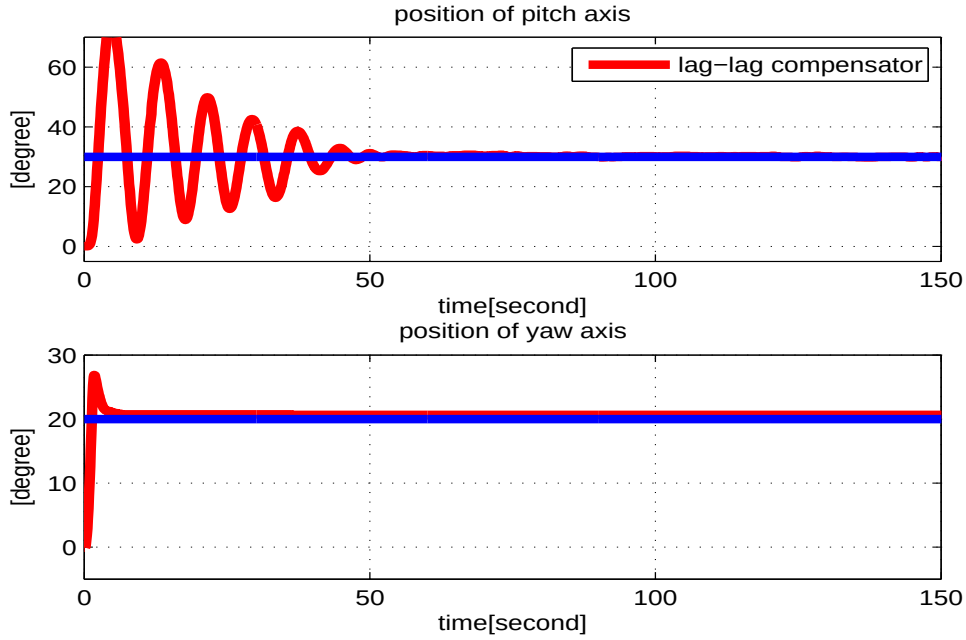

Figure 3.6. Angular pitch (top) and yaw (bottom) positions for lag-lag compensators of the form $10(\frac{s+0.1}{s+0.01})^2$ and $3000(\frac{s+0.1}{s+0.001})^2$ applied to main and tail motors, respectively

Table 3.3. Comparison of steady state errors of angular pitch and yaw positions when different controllers applied on both motors.

Controller						Steady state error					
proportional		lag		lag-lag		proportional		lag		lag-lag	
main motor	tail motor	main motor	tail motor	main motor	tail motor	pitch	yaw	pitch	yaw	pitch	yaw
10	3000	$10\frac{s+0.1}{s+0.001}$	$3000\frac{s+0.1}{s+0.001}$	$10(\frac{s+0.1}{s+0.001})^2$	$3000(\frac{s+0.1}{s+0.001})^2$	6.621	2.598	2.051	0.255	1.523	0.225
10	3000	$10\frac{s+0.1}{s+0.01}$	$3000\frac{s+0.1}{s+0.001}$	$10(\frac{s+0.1}{s+0.01})^2$	$3000(\frac{s+0.1}{s+0.001})^2$	6.621	2.598	2.139	0.412	1.875	0.4
10	3000	$10\frac{s+0.1}{s+0.02}$	$3000\frac{s+0.1}{s+0.001}$	$10(\frac{s+0.1}{s+0.02})^2$	$3000(\frac{s+0.1}{s+0.001})^2$	6.621	2.598	3.193	0.488	2.842	0.4
10	3000	$10\frac{s+0.1}{s+0.03}$	$3000\frac{s+0.1}{s+0.001}$	$10(\frac{s+0.1}{s+0.03})^2$	$3000(\frac{s+0.1}{s+0.001})^2$	6.621	2.598	3.896	0.664	3.721	0.4
10	3000	$10\frac{s+0.1}{s+0.04}$	$3000\frac{s+0.1}{s+0.001}$	$10(\frac{s+0.1}{s+0.04})^2$	$3000(\frac{s+0.1}{s+0.001})^2$	6.621	2.598	4.16	1.104	3.984	0.488

3.5. Conclusions

In this chapter, lag type compensation which significantly improves steady state error when compared with proportional controllers was presented. The theoretical results were first verified by numerical calculations and then with experimental results obtained from the twin rotor system in our laboratory where reduced steady state errors were observed.

CHAPTER 4

LEAD COMPENSATION

In this chapter, definition and important properties of lead compensation are discussed. Experiment results when these compensators applied to the twin rotor system are then given. Finally, conclusions are provided.

4.1. Definition and Properties of Lead Compensator

Lead compensator is a compensator type that is used instead of PD or PID controllers. Some disadvantages of the mentioned controllers can usually be eliminated by the assistance of a lead compensator. Sensor noise amplifying that may be caused by a derivative controller, higher control efforts that may be caused by an integral controller can be considered among these disadvantages. The main principle of a lead compensator is based on phase leading of the sinusoidal input signal Franklin et al. (1998). Lead compensator also provides better low pass filter property when compared with PID control due to this main principle. Improving the transient response of the system is the main purpose of lead compensator and this is realized by increasing the phase of open loop system which is another capability of lead compensator.

General structure of the transfer function of lead compensator is expressed in two different manners that are given as

$$D(s) = K\frac{s - z_0}{s - p_0} \tag{4.1}$$

$$D(s) = \frac{a_1 s + a_0}{b_1 s + 1} \tag{4.2}$$

where K, z_0, p_0 are gain, zero and pole of the system, respectively, and a_0, a_1, b_1 are constants that can be written in terms of K, z_0 and p_0, or vice versa. In general, designs are usually established on the following transfer function type

$$D(s) = K\frac{s + a}{s + b} \tag{4.3}$$

which is very similar to (4.1) with $a = -z_0$ and $b = -p_0$. .

As it was said before, improving the transient response is the main aim of the lead compensator design and this aim can be achieved by changing rise time, settling time,

overshoot, gain/phase margin or damping ratio that determine the behavior of transient response. Since these adjustments affect the pole locations of the controlled system it is clear that lead compensator changes the root locus. As a natural result of these, pole-zero locations become important in lead compensator design. Providing relatively fast response without losing the stability is the first aspect that must be considered while selecting these locations. In other words, a dominant pole placed in the left–half–plane must be selected. In addition to these, the zero z_0 must be closer to the origin than the pole p_0 which is the mandatory condition of lead compensator design (*i.e.*, $|z_0| < |p_0|$ in (4.1)). In this thesis study, among other transient response characteristics overshoot is considered to be the characteristic of the twin rotor system that is focused on.

4.2. Experimental Results

In this section, the experimental results obtained from the twin rotor system are presented for different lead compensators. Several lead compensators are applied to control angular pitch and yaw positions.

The experiments were conducted for 100 seconds and the desired pitch and yaw angular positions were set as 30 and 20 degrees, respectively. In these experiments, only the pole of the lead compensator for main motor was varied while keeping other control parameters unchanged. The tail motor compensator was kept the same during the experimental studies. The overshoot in pitch axis is evaluated and presented in Table 4.1. It was observed that when the pole of the lead compensator moves away from the imaginary axis, the overshoot in pitch axis decreases. The first 12 seconds of the experiment results for the lead compensators in Table 4.1 are demonstrated in Figure 4.1

4.3. Conclusions

In this chapter, to decrease the significant amount of overshoot observed in lag compensation, lead compensators were designed and experimentally evaluated on the twin rotor systems. By changing the location of the pole of the lead compensator, overshoot in pitch axis was decreased.

Table 4.1. Comparison of overshoot in angular pitch position and percentage for different lead compensators applied on the main motor.

Lead Compensator		Overshoot	Percentages of Overshoot
main motor	tail motor	pitch	pitch
$0.1\frac{s+10}{s+30}$	$600\frac{s+10}{s+20}$	33.9	% 113
$0.1\frac{s+10}{s+31}$	$600\frac{s+10}{s+20}$	31.96	% 106.53
$0.1\frac{s+10}{s+32}$	$600\frac{s+10}{s+20}$	31.88	% 106.266
$0.1\frac{s+10}{s+33}$	$600\frac{s+10}{s+20}$	30.47	% 101.56
$0.1\frac{s+10}{s+34}$	$600\frac{s+10}{s+20}$	30.03	% 100.1
$0.1\frac{s+10}{s+35}$	$600\frac{s+10}{s+20}$	29.68	% 98.93
$0.1\frac{s+10}{s+36}$	$600\frac{s+10}{s+20}$	29.41	% 98.03
$0.1\frac{s+10}{s+37}$	$600\frac{s+10}{s+20}$	26.95	% 89.83
$0.1\frac{s+10}{s+38}$	$600\frac{s+10}{s+20}$	25.37	% 84.56
$0.1\frac{s+10}{s+39}$	$600\frac{s+10}{s+20}$	23.61	% 78.7
$0.1\frac{s+10}{s+40}$	$600\frac{s+10}{s+20}$	18.25	% 60.83
$0.1\frac{s+10}{s+45}$	$600\frac{s+10}{s+20}$	15.88	% 52.93
$0.1\frac{s+10}{s+50}$	$600\frac{s+10}{s+20}$	15.18	% 50.6

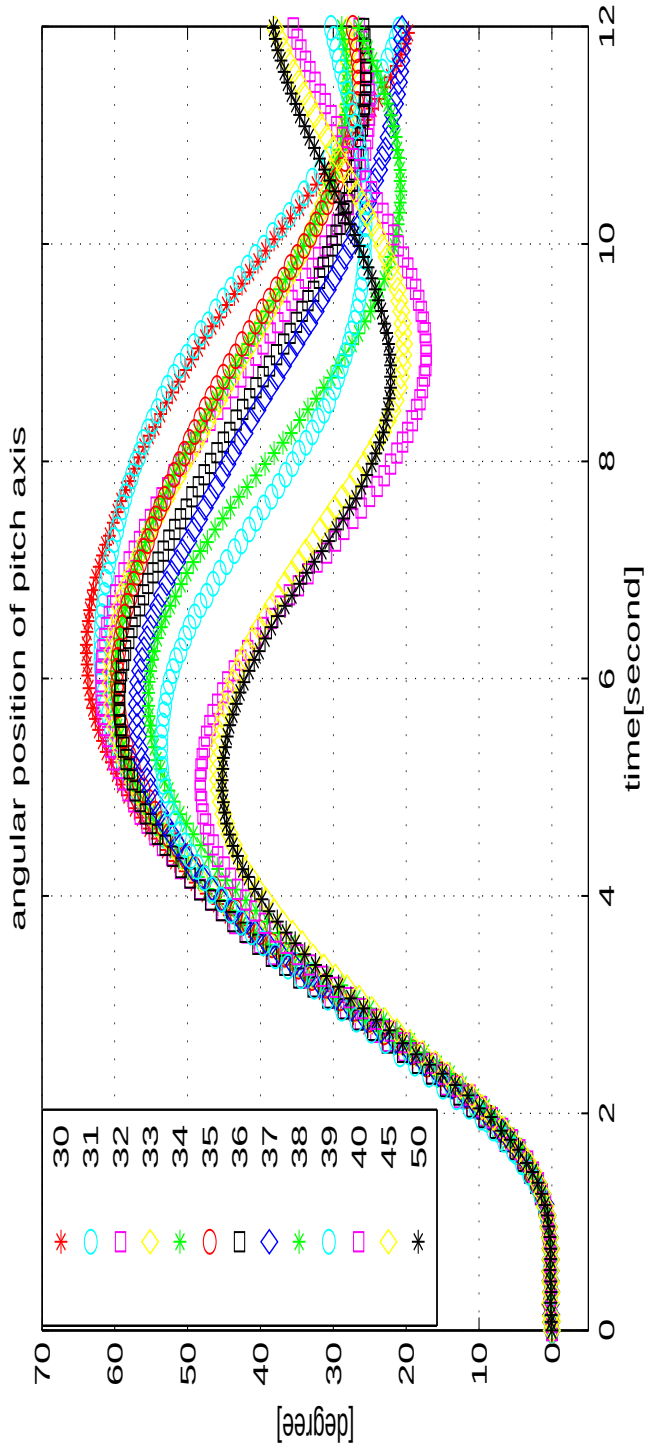

Figure 4.1. Demonstration of comparison of overshoot in pitch axis for different lead compensators.

CHAPTER 5

LAG-LEAD COMPENSATION

In this chapter, first the definition and main properties of lag-lead compensators are given. Next experiments performed on the twin rotor system are presented followed by the conclusions.

5.1. Definition and Properties of Lag-Lead Compensator

As it was mentioned in a detailed manner in the previous chapters of this thesis, both lag and lead compensators have positive effects on the different parts of system performance. It can be summarized as lead compensator doesn't affect the steady state performance while improving the transient response, and lag compensator improves the steady state performance while slowing down the transient response Franklin et al. (1998). As a result of these, using the two together is seen a useful solution to alter the transient response of a system while improving its steady state response. Since it proposes satisfactory solutions for possible problems of PID control such as saturation, noise amplifying, integrator windup and ensures better low pass filter characteristic than PID controller lag-lead compensator is preferred instead of PID controllers in control systems. One disadvantage of lag-lead compensators is that the order of the system is increased as a result of two new poles and two new zeros.

Transfer function of the lag-lead compensator contains the transfer functions of both lag and lead compensators with same properties and expressed as

$$D(s) = K\frac{s+a}{s+b}\frac{s+c}{s+d} \tag{5.1}$$

where K is the gain of the compensator, $\frac{s+a}{s+b}$ is the lead part and $\frac{s+c}{s+d}$ is the lag part.

5.2. Experimental Results

In this section, experiment results obtained from the twin rotor system by using lag-lead compensators are presented. Lag-lead compensators were designed to drive angular pitch and yaw positions to desired angular positions chosen as 30 degrees and 20

degrees, respectively. In the design of the lag-lead compensators, lead compensators from Chapter 4 are focused with the lag part was chosen as $\frac{s+0.1}{s+0.001}$ which was one of the lag compensators from Chapter 3.

The steady state error performances of the lag-lead compensators were compared with the lead compensators. The results are given in Table 5.1, from which it is clearly seen that the addition of lag compensators had a decreasing affect in steady state error.

Table 5.1. Comparison of steady state errors for lag-lead compensators compared with lead compensators applied on both motors.

Lead compensator		Steady state error	Lag-lead compensator		Steady state error
main motor	tail motor	pitch axis	main motor	tail motor	pitch axis
$0.1\frac{s+10}{s+30}$	$600\frac{s+10}{s+20}$	5.5	$0.1\frac{s+10}{s+30}\frac{s+0,1}{s+0,001}$	$600\frac{s+10}{s+20}\frac{s+0,1}{s+0,001}$	3.5
$0.1\frac{s+10}{s+31}$	$600\frac{s+10}{s+20}$	6.7	$0.1\frac{s+10}{s+31}\frac{s+0,1}{s+0,001}$	$600\frac{s+10}{s+20}\frac{s+0,1}{s+0,001}$	4.42
$0.1\frac{s+10}{s+32}$	$600\frac{s+10}{s+20}$	2.6	$0.1\frac{s+10}{s+32}\frac{s+0,1}{s+0,001}$	$600\frac{s+10}{s+20}\frac{s+0,1}{s+0,001}$	2.14
$0.1\frac{s+10}{s+33}$	$600\frac{s+10}{s+20}$	5.6	$0.1\frac{s+10}{s+33}\frac{s+0,1}{s+0,001}$	$600\frac{s+10}{s+20}\frac{s+0,1}{s+0,001}$	3.1
$0.1\frac{s+10}{s+34}$	$600\frac{s+10}{s+20}$	10.3	$0.1\frac{s+10}{s+34}\frac{s+0,1}{s+0,001}$	$600\frac{s+10}{s+20}\frac{s+0,1}{s+0,001}$	6.21
$0.1\frac{s+10}{s+35}$	$600\frac{s+10}{s+20}$	4.5	$0.1\frac{s+10}{s+35}\frac{s+0,1}{s+0,001}$	$600\frac{s+10}{s+20}\frac{s+0,1}{s+0,001}$	4.01
$0.1\frac{s+10}{s+36}$	$600\frac{s+10}{s+20}$	3.2	$0.1\frac{s+10}{s+36}\frac{s+0,1}{s+0,001}$	$600\frac{s+10}{s+20}\frac{s+0,1}{s+0,001}$	2.9
$0.1\frac{s+10}{s+37}$	$600\frac{s+10}{s+20}$	9.7	$0.1\frac{s+10}{s+37}\frac{s+0,1}{s+0,001}$	$600\frac{s+10}{s+20}\frac{s+0,1}{s+0,001}$	7.9
$0.1\frac{s+10}{s+38}$	$600\frac{s+10}{s+20}$	5.9	$0.1\frac{s+10}{s+38}\frac{s+0,1}{s+0,001}$	$600\frac{s+10}{s+20}\frac{s+0,1}{s+0,001}$	5.5
$0.1\frac{s+10}{s+39}$	$600\frac{s+10}{s+20}$	10.5	$0.1\frac{s+10}{s+39}\frac{s+0,1}{s+0,001}$	$600\frac{s+10}{s+20}\frac{s+0,1}{s+0,001}$	3.2
$0.1\frac{s+10}{s+40}$	$600\frac{s+10}{s+20}$	9.08	$0.1\frac{s+10}{s+40}\frac{s+0,1}{s+0,001}$	$600\frac{s+10}{s+20}\frac{s+0,1}{s+0,001}$	6.01
$0.1\frac{s+10}{s+45}$	$600\frac{s+10}{s+20}$	7.76	$0.1\frac{s+10}{s+45}\frac{s+0,1}{s+0,001}$	$600\frac{s+10}{s+20}\frac{s+0,1}{s+0,001}$	4.1
$0.1\frac{s+10}{s+50}$	$600\frac{s+10}{s+20}$	12.86	$0.1\frac{s+10}{s+50}\frac{s+0,1}{s+0,001}$	$600\frac{s+10}{s+20}\frac{s+0,1}{s+0,001}$	5.04

5.3. Conclusions

In this chapter, to make use of the good properties of lag and lead compensators, lag-lead compensators were introduced. Experiments performed on the twin rotor system were demonstrated where improved steady state error was observed when compared with only led compensation.

CHAPTER 6

CONCLUSIONS

In this thesis study, modeling and control of the twin rotor system in our laboratory were investigated. Firstly, via utilizing experimentally collected data, two input-output models of the twin rotor system were obtained. Artificial neural networks were utilized to obtain the first model which was in the time domain. The second model was a transfer function model in the Laplace domain which was developed by using Matlab System Identification Toolbox.

The remaining part of this thesis was devoted to designing lag and lead compensators and their experimental verification. Firstly, lag compensators, which are commonly utilized to decrease steady state errors without changing the transient characteristics much, were designed. Several experiments were conducted that demonstrated the proof of concept.

Lead compensation was considered next to decrease the high amount of overshoot that was observed in most of the experiments performed on the twin rotor system. A good amount of reduction in overshoot was achieved via changing the location of the pole of the lead compensator.

Finally, in Chapter 5, to achieve reduced overshoot while at the same time decreasing the steady state errors, lag and lead compensators were fused to yield lag-lead compensation. Experimental results confirmed that reduced steady state error was obtained when lag compensator was used in conjuction with lead compensator.

When compared with the existing literature on twin rotor systems the main novelty of this thesis study according to our best knowledge is that lag and lead type compensation techniques were for the first time, applied to twin rotor systems to overcome the several shortcomings of PID controllers. There is much to be considered as future work.

- One of the main shortcomings of designing controllers for twin rotor systems is that usually very less is known about their models. This affected the design of lead compensators where instead a trial and error type approach was followed. To overcome this, some line of future research may focus on obtaining more accurate and maybe nonlinear transfer function model for these systems.

- Another possible future research problem is to obtain a state space model that could

be used for numerical simulation purposes from the transfer functions in Chapter 2 to which a neural network based component, similar to the one in Chapter 2, can be added for uncertainty modeling.

- An interesting future research is to compare the experiment results obtained from the in-house developed twin rotor system with the commercially available twin rotor systems in Feedback Instruments Limited[1] and Quanser Inc.[2]. Appliying lag lead compensation to experiment test-beds with different dof may also be considered as a possible future work.

[1]Feedback Instruments Limited, Crowborough, UK. http://www.feedback-instruments.com/

[2]Quanser Inc., Ontario, Canada. http://www.quanser.com/

REFERENCES

Ahmad, S., A. Chipperfield, and M. Tokhi (2000). Dynamic modeling and optimal control of a twin rotor mimo system. In *National Aerospace and Electronics Conference, 2000. NAECON 2000. Proceedings of the IEEE 2000*, pp. 391–398. IEEE.

Ahmad, S., A. Chipperfield, and M. Tokhi (2001). Parametric modelling and dynamic characterization of a two-degree-of-freedom twin-rotor multi-input multi-output system. *Proceedings of the Institution of Mechanical Engineers, Part G: Journal of Aerospace Engineering 215*(2), 63–78.

Ahmad, S., A. Chipperfield, and M. Tokhi (2003). Dynamic modelling and linear quadratic gaussian control of a twin-rotor multi-input multi-output system. *Proceedings of the Institution of Mechanical Engineers, Part I: Journal of Systems and Control Engineering 217*(3), 203–227.

Ahmad, S., A. Chipperfield, and M. Tokhi (2004). Dynamic modelling and open-loop control of a two-degree-of-freedom twin-rotor multi-input multi-output system. *Proceedings of the Institution of Mechanical Engineers, Part I: Journal of Systems and Control Engineering 218*(6), 451–463.

Alagoz, B. B., A. Ates, and C. Yeroglu (2013). Hata-kupu kontrol yapisinin teorik incelenmesi. In *National Conference of Turkish National Comitee of Automatic Control*, pp. 836–841.

Bayrak, A., F. Dogan, E. Tatlicioglu, and B. Ozdemirel (2015). Design of an experimental twin-rotor multi-input multi-output system. *Computer Applications in Engineering Education 23*, 578–586.

Bayrak, A., M. Salah, N. Nath, and E. Tatlicioglu (2010). Neural network-based nonlinear control design for twin rotor mimo systems. In *Proc. of Int. Symposium on Mechanism and Machine Science*, pp. 172–178.

Corradini, M. L., A. Cristofaro, and G. Orlando (2011). Stabilization of discrete-time linear systems with saturating actuators using sliding modes: Application to a twin-rotor system. In *Decision and Control and European Control Conference (CDC-*

ECC), 2011 50th IEEE Conference on, pp. 8237–8242. IEEE.

Czajkowski, A. (2014). Robust control with disturbance estimation using echo state networks for the twin rotor aero-dynamical system application? In *19th World Congress The International Federation of Automatic Control*, pp. 11305–11310.

Deniz, M., K. M. Dogan, E. Tatlicioglu, and A. Bayrak (2014). Cift rotorlu cok girisli cok cikisli sistem icin gürbüz denetleyici tasarımı ve gerceklenmesi. In *National Conference of Turkish National Comitee of Automatic Control*, pp. 511–516.

Dogan, F. (2014). Design, development and control of a twin rotor system. Master's thesis, Izmir Institute of Technology.

Dogan, F., B. Bidikli, A. Bayrak, and E. Tatlicioglu (2012). Cift rotorlu sistemin gürbüz denetlenmesi. In *National Conference of Turkish National Comitee of Automatic Control*, pp. 127–131.

Dong, X., X. Zhao, and M. Shu (2008). Research of control method based on 3-dof twin rotor mimo system. In *Intelligent Control and Automation, 2008. WCICA 2008. 7th World Congress on*, pp. 3279–3283. IEEE.

Dorf, R. C. and R. H. Bishop (1998). *Modern control systems*. Pearson (Addison-Wesley).

Franklin, G. F., J. D. Powell, and M. L. Workman (1998). *Digital control of dynamic systems*, Volume 3. Addison-Wesley.

Juang, J.-G., M.-T. Huang, and W.-K. Liu (2008). Pid control using presearched genetic algorithms for a mimo system. *Systems, Man, and Cybernetics, Part C: Applications and Reviews, IEEE Transactions on 38*(5), 716–727.

Juang, J.-G., W.-K. Liu, and C.-Y. Tsai (2005). Intelligent control scheme for twin rotor mimo system. In *Mechatronics, 2005. ICM'05. IEEE International Conference on*, pp. 102–107. IEEE.

Juang, J.-G., K.-T. Tu, and W.-K. Liu (2006). Hybrid intelligent pid control for mimo system. In *Neural Information Processing*, pp. 654–663. Springer.

Karimi, H. R. and M. R. J. Motlagh (2006). Robust feedback linearization control for a non linearizable mimo nonlinear system in the presence of model uncertainties. In *Service Operations and Logistics, and Informatics, 2006. SOLI'06. IEEE International Conference on*, pp. 965–970. IEEE.

Liu, C.-S., L.-R. Chen, B.-Z. Li, S.-K. Chen, and Z.-S. Zeng (2006). Improvement of the twin rotor mimo system tracking and transient response using fuzzy control technology. In *Industrial Electronics and Applications, 2006 1ST IEEE Conference on*, pp. 1–6. IEEE.

López-Martinez, M., M. G. Ortega, C. Vivas, and F. R. Rubio (2007). Nonlinear l2 control of a laboratory helicopter with variable speed rotors. *Automatica 43*(4), 655–661.

López-Martinez, M. and F. Rubio (2003). Control of a laboratory helicopter using feedback linearization. In *European Control Conference (ECC-03)*, pp. 1–4.

López-Martinez, M., C. Vivas, and M. Ortega (2005). A multivariable nonlinear h_infty controller for a laboratory helicopter. In *IEEE CONFERENCE ON DECISION AND CONTROL*, Volume 44, pp. 4065. IEEE; 1998.

Lu, T.-W. and P. Wen (2007). Time optimal and robust control of twin rotor system. In *Control and Automation, 2007. ICCA 2007. IEEE International Conference on*, pp. 862–866. IEEE.

Mustafa, G. and N. Iqbal (2004). Controller design for a twin rotor helicopter model via exact state feedback linearization. In *Multitopic Conference, 2004. Proceedings of INMIC 2004. 8th International*, pp. 706–711. IEEE.

Ocal, Z. and Z. Bingul (2013a). Iki serbestlik dereceli helikopter sisteminin modellenmesi ve parametrelerin genetik algoritma yardımıyla belirlenmesi. In *National Conference of Turkish National Comitee of Automatic Control*, pp. 525–530.

Ocal, Z. and Z. Bingul (2013b). İki serbestlik dereceli helikopter sisteminin ters model tabanlı kontrolü. In *National Conference of Turkish National Comitee of Automatic Control*, pp. 366–370.

Radac, M.-B., R.-C. Roman, R.-E. Precup, and E. M. Petriu (2014). Data-driven model-free control of twin rotor aerodynamic systems: Algorithms and experiments. In *Intelligent Control (ISIC), 2014 IEEE International Symposium on*, pp. 1889–1894. IEEE.

Rahideh, A., H. Shaheed, and A. H. Bajodah (2007). Adaptive non-linear model inversion control of a twin rotor multi-input multi-output system using artificial intelligence. *Proceedings of the Institution of Mechanical Engineers, Part G: Journal of Aerospace Engineering 221*(3), 343–351.

Rahideh, A. and M. Shaheed (2006). Hybrid fuzzy-pid-based control of a twin rotor mimo system. In *IEEE Industrial Electronics, IECON 2006-32nd Annual Conference on*, pp. 48–53. IEEE.

Rahideh, A., M. Shaheed, and H. Huijberts (2008). Dynamic modelling of a trms using analytical and empirical approaches. *Control Engineering Practice 16*(3), 241–259.

Rahideh, A. and M. H. Shaheed (2008). Dynamic modelling of a twin rotor mimo system using grey box approach. In *Mechatronics and Its Applications, 2008. ISMA 2008. 5th International Symposium on*, pp. 1–6. IEEE.

Shaheed, H. M. (2005). Feedforward neural network based non-linear dynamic modelling of a trms using rprop algorithm. *Aircraft Engineering and Aerospace Technology 77*(1), 13–22.

Shih, C.-L., M.-L. Chen, and J.-Y. Wang (2008). Mathematical model set-point stabilizing controller design of a twin rotor mimo system. *Asian journal of control 10*(1), 107–114.

Su, J.-P., C.-Y. Liang, and H.-M. Chen (2002). Robust control of a class of nonlinear systems and its application to a twin rotor mimo system. In *Industrial Technology, 2002. IEEE ICIT'02. 2002 IEEE International Conference on*, Volume 2, pp. 1272–1277. IEEE.

Tahir, F., Q. Ahmed, and A. I. Bhatti (2013). Real-time switched model predictive control of a twin rotor system. In *Decision and Control (CDC), 2013 IEEE 52nd*

Annual Conference on, pp. 4847–4852. IEEE.

Toha, S. and M. Tokhi (2008). Mlp and elman recurrent neural network modelling for the trms. In *Cybernetic Intelligent Systems, 2008. CIS 2008. 7th IEEE International Conference on*, pp. 1–6. IEEE.

Witczak, P., M. Witczak, K. Patan, and R. Stetter (2014). Design of robust predictive fault-tolerant control for takagi-sugeno fuzzy systems: Application to the twin-rotor system. In *Intelligent Control (ISIC), 2014 IEEE International Symposium on*, pp. 1113–1118. IEEE.